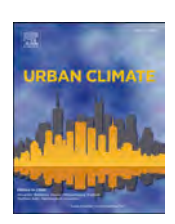


Contents lists available at ScienceDirect

Urban Climate

journal homepage: www.elsevier.com/locate/uclim





Spatial-temporal modeling of the relationship between surface temperature and air temperature in metropolitan urban systems

Madeline Scolio a,*, Peleg Kremer , Yimin Zhang b, Kabindra M. Shakya

ARTICLE INFO

Keywords: Air temperature Surface temperature Spatiotemporal modeling Spatial autocorrelation Temporal autocorrelation Urban heat

ABSTRACT

Research about urban local climate and urban heat island often relies on land surface temperature (LST) data to characterize the distribution of temperature near the surface. Although using remotely sensed data for such work has the advantage of continuous spatial coverage at regular temporal intervals, it is recognized that surface temperature is not an ideal proxy for air temperature (AT). This study's goal is to develop a spatiotemporal model revealing the relationship between LST and AT within the complexities of the urban environment. A mobile weather monitoring unit was used to collect spatially-explicit fine-scale AT data while Landsat 8 and 9 passed overhead collecting LST data. A spatiotemporal model of the relationship between LST and AT in Philadelphia was constructed with this data utilizing basis functions to account for spatial and temporal autocorrelation. The spatiotemporal model results show a strong relationship between LST and AT and indicate that it is possible to predict fine scale AT (120 m) using remotely sensed LST in an urban context (r-squared = 0.99, RMSE = 0.89 °C). The spatiotemporal model outperforms models that do not account for spatial and temporal autocorrelation, highlighting the importance of considering these dependencies in temperature modeling. City-wide AT predictions were generated for Philadelphia demonstrating the ability of the model to improve understanding of local urban climate.

1. Introduction

As climate change causes global temperatures to rise (Calvin et al., 2023) and urbanization continues to intensify (Huang et al., 2019), there is a growing concern for the burden of heat in cities (Greene et al., 2011; Harlan and Ruddell, 2011). It is a common practice to use remotely sensed land surface temperature (LST) as a proxy for air temperature (AT) in studies of local urban climate and urban heat island (Buyantuyev and Wu, 2010; Ho et al., 2016; Hondula and Davis, 2014). AT refers to the temperature of the air, usually 2 m above the land surface, at a given location whereas LST refers to the temperature of the land surface at a given location. It is recognized that satellite derived remotely sensed LST is not a perfect proxy for AT due to many limitations, such as limited sampling frequency and cloud cover obscuration (Berg and Kucharik, 2022). In urban areas, LST is unable to accurately account for the physical heterogeneity of the built environment (Meili et al., 2021). Furthermore, the actual temperature of the air differs from LST due to humidity, wind, and the capacity of surface to retain heat (Stewart et al., 2021). In urban contexts, where social and physical environments change rapidly across space and time, LST lacks critical nuance and precision to accurately reflect fine scale temperature

^a Department of Geography and the Environment, Villanova University, PA, USA

^b Department of Mathematics and Statistics, Villanova University, PA, USA

^{*} Corresponding author at: Department of Geography & the Environment, Villanova University, 800 Lancaster Avenue, Villanova, PA 19085, USA. *E-mail address*: Mscolio@villanova.edu (M. Scolio).

patterns and the lived experience of community members (White, -Newsome Jalonne L., Brines, S. J., Brown, D. G., Dvonch, J. T., Gronlund, C. J., Zhang, K., Oswald, E. M., and O, 'Neill Marie S., 2013).

AT data is collected using monitors that can record data for the specific times and locations where they are active. AT data is often collected at weather stations sporadically distributed in point locations such as airports. Some cities, like Madison, WI (Berg and Kucharik, 2022); Novi Sad City, Serbia (Savić et al., 2023); and Birmingham, UK (Warren et al., 2016), have extensive stationary AT monitoring networks, but these are difficult and costly to maintain in the long term and still provide limited spatial coverage. Spatially sporadic weather data has limited usefulness in spatial analysis of urban systems where extreme heterogeneity requires fine spatial analysis (Sohrabinia et al., 2015). Mobile monitoring has been used in some studies to obtain accurate AT data. While researchers have launched successful data collection campaigns with temperature sensors mounted to backpacks (Schwarz et al., 2012), bikes (Ziter et al., 2019), and cars (Unger et al., 2010), mobile monitoring is also restricted in spatial scope and has limited capability to produce a long historical record. In effect, the lack of availability of fine scale AT data has inhibited research on how AT influences and is influenced by urban systems.

LST is commonly measured through remote sensing such as thermal sensors on satellite platforms. The LANDSAT satellites monitor LST at a relatively fine spatial and temporal resolution (Sohrabinia et al., 2015). For example, Landsat satellites 8 and 9 measure the surface temperature of a location every 8 days at 100-m resolution (Landsat Science Products, 2023). LST is measured using thermal infrared sensors (TIRS). LST is calculated by applying the Single Channel algorithm on TIRS Band 10 (Landsat Science Products, 2023). The Landsat 8 thermal sensors Band 10 measure wavelengths from 10.6 to 11.2 μ m (Lloyd, 2021) while the Landsat 9 thermal sensors Band 10 measure wavelengths 10.3–11.3 μ m (Landsat 9 Bands, 2021).

A major limitation of using LST data remotely sensed from satellites is that cloud cover affects the quality and spatial extent of the data. Thermal infrared sensors cannot penetrate clouds meaning their data is only viable on days with limited to no cloud cover. Efforts have been made to develop methodologies to correct for cloud cover interference, but no consensus on best practice has been reached (Wang et al., 2019; Zhu et al., 2022). LST is also limited temporally because it is measured at specific days and times. For example, Landsat satellites pass over Philadelphia every 8 days around 11:40 am EST (Landsat Science Products, 2023). In contrast, weather stations measuring AT operate continuously providing better temporal resolution. Whereas AT monitors can measure temperature at a specific location, remotely sensed LST has a coarser resolution and generalizes temperatures over a unit of distance. Landsat satellites 8 and 9 measure LST at 100 m resolution (Landsat 9 Bands, 2021; Lloyd, 2021).

LST data is commonly used to represent temperature in a myriad of different applications. Many studies of urban heat island (UHI) focus on surface urban heat island (SUHI) using LST data because of its accessibility and large spatial coverage (Liu et al., 2016). Further, LST is often used to show changes in climate patterns due to the large historical catalog of LST data (Pepin et al., 2019). LST has also been used to measure how changes in landcover and urban structure impact temperatures (Julien et al., 2011; Lemoine-Rodríguez et al., 2022; Li et al., 2016; Mitz et al., 2021; Mumtaz et al., 2020; J. D. Stewart and Kremer, 2022). In studies of the impact of temperature on human health and heat vulnerability, it is also common to use LST due to the widely accessible nature of this data (Navarro-Estupiñan et al., 2020; Schinasi et al., 2022). Nevertheless, researchers recognize that in most cases using LST data is not ideal and further measures should be developed to improve temperature data quality and availability (Stewart et al., 2021).

The relationship between surface temperature and air temperature is understood to be highly specific to time, location and scale. Generally, LST has larger diurnal variability than AT, with higher daytime temperatures and lower nighttime temperatures (Sohrabinia et al., 2015; White-Newsome et al., 2014). The relationship between LST and AT has been demonstrated to be stronger at night than during the day (Goldblatt et al., 2021; Shiflett et al., 2017). The difference between AT and LST is greatest when both are highest during the summer and early afternoon (Gallo et al., 2011; Zhang et al., 2014). This relationship has been studied around the globe at geographic scales that span from continents (Chakraborty et al., 2022; Zhang et al., 2014) to neighborhoods (Goldblatt et al., 2021; Unger et al., 2010). Typically, there is a strong relationship between LST and AT in homogeneous rural settings, but other factors like cloud cover, wind, time of day, season, and nearby land cover can affect this relationship (Gallo et al., 2011; Mutiibwa et al., 2015).

The heterogeneity of urban environments further complicates the relationship between AT and LST. Confounding factors that are specific to the natural and built environment of a site impact how LST and AT relate to each other meaning that this relationship can vary greatly from city to city (Naserikia et al., 2023; Yoo et al., 2018). As urban areas are all unique, research on this relationship has yielded different results depending on the city. Studies in Vancouver, Canada and Hangzhou, China found either poor or no correlations between LST and AT although these studies faced AT data limitations (Ho et al., 2016; Sheng et al., 2017). Ho et al. (2016) relied heavily on data from Weather Underground's network of personal weather stations which is easily accessible but hindered by unreliable accuracy and precision of the data. Sheng et al. (2017) managed their own network of five weather stations but were limited in spatial extent due to the small number of stations. Nevertheless, a growing number of studies in cities across the world find a correlation between LST and AT. These studies relied on large networks of stationary monitors (Alvi et al., 2022; Azevedo et al., 2016; do Nascimento, A. C. L., Galvani, E., Gobo, J. P. A., and Wollmann, C. A., 2022; Sfîcă, and Creţu, C.-Ştefānel, Ichim, P., Hriţac, R., and Breabăn, I.-G., 2023), extensive mobile monitoring (Amani-Beni et al., 2022; Unger et al., 2010) or a combination of both (Schwarz et al., 2012) in order to compile large quantities of AT data needed for accurate modeling. However, many of these studies have attempted to investigate a linear relationship between AT and LST which may be inappropriate given the complexity of the urban environment and how it affects temperatures.

The essential issue of spatiotemporal analysis is that observations collected close in time and space are related (Tobler, 1970). This violates the assumption of independence that is foundational to linear analysis. Failure to address spatial and temporal dependence in variables can lead to biased regression estimates or greater standard errors in the regression estimators, which impacts the validity of statistical inference. It has been established that spatial and temporal autocorrelation are present in both LST and AT, yet recent research suggests that climate change could increase both spatial and temporal autocorrelation of temperature underscoring the

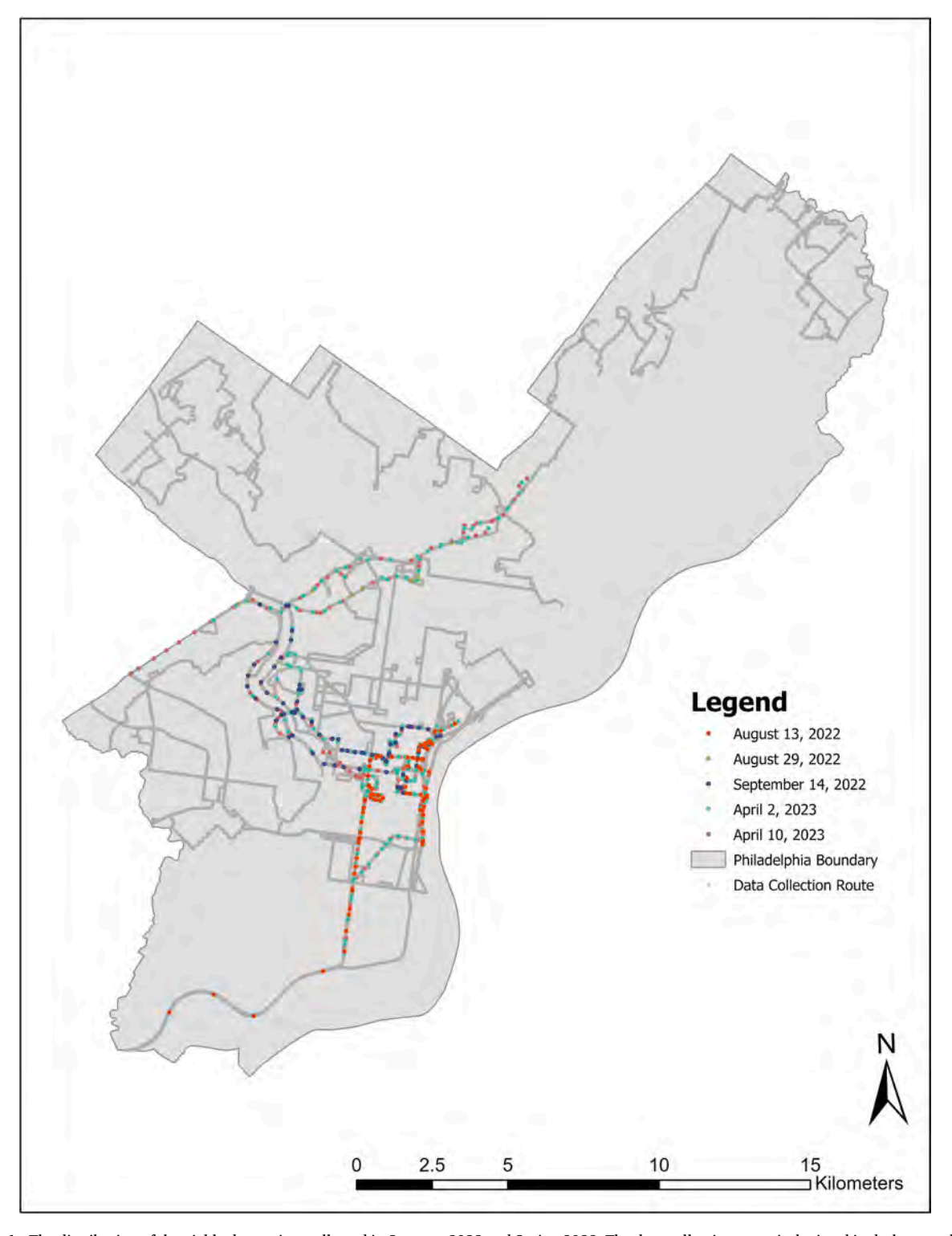


Fig. 1. The distribution of the viable data points collected in Summer 2022 and Spring 2023. The data collection route is depicted in dark grey while viable points from each day are shown in orange, green, blue, teal, and mauve. (For interpretation of the references to colour in this figure legend, the reader is referred to the web version of this article.)

importance of developing methodologies for accounting for these effects (Di Cecco and Gouhier, 2018). Spatially regressive models, like spatial lag and spatial error models, account for spatial autocorrelation in various ways to correct the independence assumption violation inherent to spatial data (Ward and Gleditsch, 2019). Spatiotemporal models account for both spatial and temporal dependence in the data. Spatiotemporal autocorrelation has been dealt with in autoregressive-integrated-moving-average models, space—time autoregressive models, three-dimensional geostatistical models, and panel data models (Griffith, 2010).

Models relating LST and AT in urban environments are only beginning to develop in the literature because of the complexity of modeling and the lack of appropriate empirical data. Models have been developed predicting AT from LST at larger spatial scales (e.g. 1 km) across large study areas (e.g. Northeastern USA) but few are city-specific and operate at a spatial scale that would be most useful in dense metropolitan areas (Kloog et al., 2014; Parmentier et al., 2015). Successful models have been developed with smaller scopes in other parts of the world (Emamifar et al., 2013; Sandoval and Meza, 2014; W. Zhu et al., 2013). However, these models focus on rural areas. Alvi et al. (2022) produced a model able to predict fine scale AT across an urban environment using only LST, land cover and emissivity data, but their model does not account for spatial and temporal autocorrelation. Machine learning based models are also beginning to develop and show promising predictive results (dos Santos, 2020). Currently, we are unaware of any other studies that successfully predict AT using only LST at a fine scale accounting for both spatial and temporal autocorrelation in the model itself within an urban system.

This study aims to investigate the AT-LST relationship in urban areas by creating a spatiotemporal model of AT, applied in Philadelphia, PA. Overall, the goal is to provide a better understanding of the relationship between LST and AT in the urban environment in order to support efforts to improve our collective knowledge on temperature interactions in urban systems. The objectives of this study are as follows: a) To collect significant amounts of AT data through mobile monitoring while Landsat LST is being remotely sensed. b) To create a spatio-temporal model that accounts for both spatial and temporal autocorrelation within the model structure capable of predicting spatially continuous fine scale (120 m) daily AT using only LST as an input. c) To employ the model to produce city-wide AT predictions using remotely sensed LST and to examine how AT predictions and remotely sensed LST vary over space and time.

2. Methods

2.1. Case study area: Philadelphia

Philadelphia is the largest city in Pennsylvania with a population of 1,603,797 people as of 2020 (*QuickFacts: Philadelphia City, Pennsylvania*, 2022). The city has a population density of 30,896 people per square km indicating that the city is highly urbanized and densely developed (*QuickFacts: Philadelphia City, Pennsylvania*, 2022). Landcover in Philadelphia consists primarily of high-density urban development, and projections predict that the city will gain more dense urban development in the coming years as the population continues to grow (USGS, 2019, Shade and Kremer, 2019).

Nevertheless, Philadelphia is home to many large formal green spaces as well as smaller informal green spaces like vacant lots (Pearsall, 2017). Official city parkland makes up approximately 9.3% of the city's land area (Nowak et al., 2016). According to a 2018 Tree Canopy Assessment, the city as a whole had about 20% tree canopy coverage, but this is not distributed evenly. Overall, wealthier whiter neighborhoods tend to have greater tree canopy coverage (Philly Tree Plan, 2023). Access to greenspace varies dramatically across the city and is also heavily influenced by socioeconomic status (Locke et al., 2023). Greening has been shown to be a critical component of reducing heat in urban environments meaning this inequitable distribution has serious consequences for human health and well-being (Ziter et al., 2019).

2.2. Air temperature

AT data was collected through a data collection campaign in Philadelphia during Summer 2022 (August 13, August 29, and September 14) and Spring/Summer of 2023 (April 2, April 10, and June 5). On days where the Landsat satellite passed over the city, AT data was collected for the two hours before and two hours after the satellite passed over (~11:40 am EST/15:40 GMT). A car equipped with GPS and weather monitoring equipment traveled a predetermined route traversing about 160 km representing a diverse combination of the Philadelphia urban landscape (Fig. 1).

In summer 2022, the route was split into 4 sections that were each driven once during each month of the study period while the LANDSAT satellite passed overhead. For the spring/summer 2023 campaign, a new route was created with the goal of achieving data replication at the locations of viable data points from the summer 2022 campaign.

The Davis Instruments Vantage Pro2 Weather Station was used to measure and record AT and relative humidity at one-minute intervals. The weather monitor was mounted on the back of the vehicle to eliminate any potential interference from residual heat from the engine. iPads connected to a Trimble R1 High Accuracy GPS receiver and two Bad Elf GPS Pro+ receivers were used to record time and coordinate locations at one second intervals. In the spring campaign's data collection, a Trimble TDC650 GNSS Handheld GPS unit in addition to the Trimble R1 High Accuracy GPS receiver were used to record location data. The weather data was matched with the GPS locations based off the timestamp using an R script. In cases where the timestamps did not match exactly, the weather data was matched with the closest GPS location within five seconds before or after the weather data was collected.

2.3. Land surface temperature

The USGS LANDSAT Acquisition Tool (https://landsat.usgs.gov/landsat_acq) was utilized to determine when the Landsat 8 and

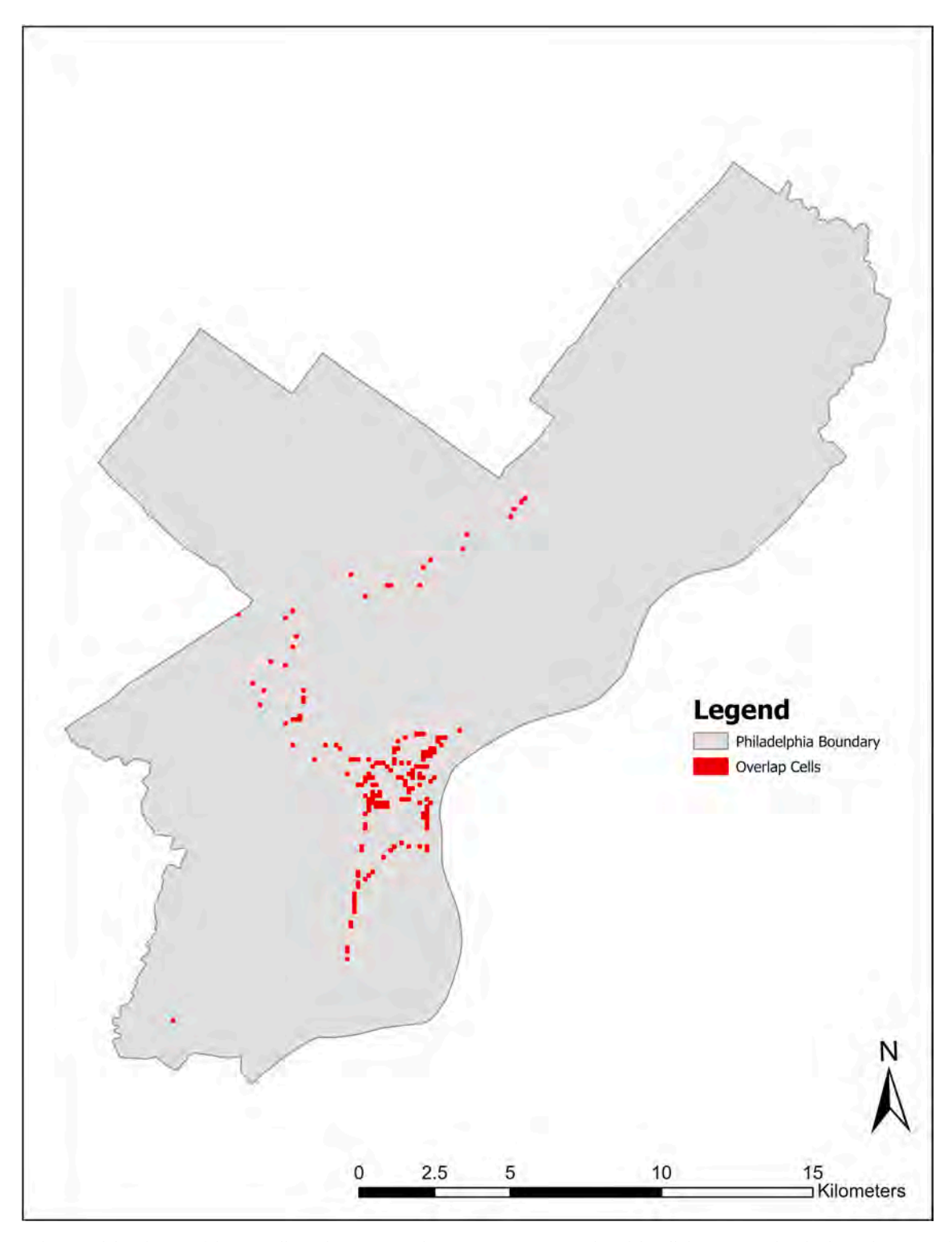


Fig. 2. The spatial distribution of the 172 cells used to construct the AT-LST spatiotemporal model. Cell that contained multiple AT data points from different days were deemed to be relevant "Overlap Cells" and are shown in red. The overlap cells are concentrated in Center City, South Philadelphia, and North Philadelphia. (For interpretation of the references to colour in this figure legend, the reader is referred to the web version of this article.)

Landsat 9 satellites passed over Philadelphia for the study period. Landsat Collection 2 level 2 LST Analysis Ready Data (ARD) thermal band data was downloaded for the satellite acquisition days and transformed to LST in °C following established procedures (Landsat Science Products, 2023). LANDSAT ARD data is atmospherically corrected and converted to surface temperature by an automated procedure allowing direct use of the data for research purposes.

2.4. Data processing

Landsat ARD pixel quality assessment raster was used to create a mask of cloud cover. For Landsat LST data, each pixel in the data raster is assigned a code that corresponds to a level of confidence that there is cloud interference as well as the type of cloud and how significant the interference is (Landsat Science Products, 2023). These codes are commonly used by researchers to filter out inaccurate data from the LST raster but in doing so some of the spatial continuity of the data is lost leading to gaps (Dwyer et al., 2018). This mask was used to eliminate any pixels that were compromised by clouds.

Davis weather data was filtered to include points that were collected within the window of two hours before and two hours after the LANDSAT pass over time (~11:40 am EST/15:40 GMT). The Davis AT data matched with GPS data was georeferenced in ArcGIS Pro using the Display XY Data tool. Since the model that was used for this analysis employed temporal basis functions, repetition of the same geographic location across multiple days was needed. A 120 m fishnet was overlayed with the points, and cells with data points from multiple days were extracted to be used for analysis. The fishnet allowed for a standardized way to determine where data points overlapped in location. In the end, 172 cells contained points on multiple days and were used in the analysis (Fig. 2).

LST was extracted and averaged from processed Landsat data for each cell. The matched LST and AT data was exported as a CSV file for analysis in R.

2.5. Data analysis

We expected to encounter some level of spatial autocorrelation in our data due to the thermodynamic nature of both LST and AT. Spatial autocorrelation refers to the amount of clustering present in a data set (Schwarz et al., 2015). To assess the level of spatial autocorrelation in our data, a univariate local Moran's I test was performed on LST and AT data using GeoDa. Since temperatures can change from day to day, the data was also grouped by collection day when performing these tests.

The same data set that was used to construct the spatiotemporal model was also used to develop Ordinary Least Squares (OLS), Spatial Lag and Spatial Error models in GeoDa for comparison. These models provided benchmarks to assess the importance of accounting spatiotemporal dependence in the data. OLS is a commonly used method for assessing the relationship between a dependent variable and one or more independent variables by estimating the coefficients of a linear regression equation that describes the relationship. Importantly, OLS does not account for spatial or temporal dependence in the data as it assumes the error terms are independent. Spatial lag and spatial error models are two commonly used spatially autoregressive models that account for spatial autocorrelation in data. Spatial lag introduces a spatially lagged dependent variable to explain the spatial effects of the dependent variable (Cliff and Ord, 1973). Eq. 1 depicts the structure of the spatial lag model:

$$y = pWy + x\beta + \varepsilon$$
 (1)

where Wy is the spatial lagged dependent variable for the weights matrix (W), p is the spatial autoregressive coefficient, x is a matrix of observations on the explanatory variables, β is the vector of regression coefficients, and ε is a vector of the error terms which is independently and identically distributed. In contrast, the spatial error model accounts for spatial dependence in the error term (Anselin, 1988). The spatial error model takes the form of:

$$y = x\beta + \varepsilon$$

$$\varepsilon = \lambda W \varepsilon + \xi$$
(2)

where, x is a matrix of observations on the explanatory variables, β is the vector of regression coefficients, ε is the vector of error terms, spatially weighted using the weights matric (W), λ is the spatial error coefficient, and ξ is a vector of uncorrelated error terms. We employ a queen contiguity-based spatial weight matrix for spatial lag and spatial error modeling.

The spatiotemporal model employed in this research was adapted from the work of Fuentes and Guttorp (2006) and Wikle et al. (2019) and utilizes the R package SpatioTemporal developed by Lindström et al. (2013). The structure of the model is:

$$Y(s;t) = x(s;t)'\beta + \sum_{i=1}^{n_{a}} \phi_{i}(t)\alpha_{i}(s) + v$$
(3)

Y(s;t) refers to the spatiotemporal observations meaning the air temperature at location s and time t. In the first term, x(s;t) is the spatiotemporal covariate and β is the regression coefficient. Latitude and longitude data for the center of each cell served as geographic covariates, s, while surface temperature served as the spatiotemporal covariate, x(s;t), with t representing the date on which the data was collected. The dates from which we observe data are discrete. The dates were reformatted to account for seasonal effects by assigning a value of 1 to the date earliest in the calendar year (in this case, August 2nd, 2023) and using a day counter to assign values to other dates based on their distance from the first date. In the second term, $\{\Phi_t(t)\}$ are the data-driven temporal basis functions which

use smoothed empirical orthogonal functions (Fuentes and Guttorp, 2006) to account for temporal autocorrelation, and $\{\alpha_i(s)\}$ are the coefficients of the temporal basis functions are used to account for spatial autocorrelation. ν is independently and identically distributed with a fixed variance, σ^2 , across space and time.

Temperature, collection dates and location data were used to estimate the temporal basis functions and their coefficients to account for temporal and spatial correlation. Temporal autocorrelation between the observed days is accounted for solely by the temporal basis functions $\{\Phi_f(t)\}$. The prediction of the temporal basis function values at unobserved days is done through spline interpolation. The benefits of using basis functions include simplifying model parameters for estimation and gaining computational advantage via flexible basis function design. This model employs two temporal basis functions to best fit the data, but additional basis functions can be added depending on the data being used. Spatial autocorrelation is accounted for by the alpha coefficients of the basis function which are modeled as multivariate (spatial) random fields. The $\{\alpha_i(s)\}$ is a Gaussian random variable of which the mean is a function of the spatial covariates. However, to avoid model overfitting, in our model the means of the basis function coefficients are chosen as constants, independent of geographic covariates. Our model allows temporal correlations to vary with spatial locations via the $\{\alpha_i(s)\}$. The covariance between $\{\alpha_i(s)\}$ at two different locations decays following an exponential function as distance increases between the two locations shown in eq. 4:

$$E(\alpha_{1}(\mathbf{s})) = \alpha_{1}, cov(\alpha_{1}(\mathbf{s}), \alpha_{1}(\mathbf{s} + \mathbf{h})) = \sigma_{1}^{2} exp\left(-\frac{\|\mathbf{h}\|}{r_{1}}\right)$$

$$E(\alpha_{2}(\mathbf{s})) = \alpha_{2}, cov(\alpha_{2}(\mathbf{s}), \alpha_{2}(\mathbf{s} + \mathbf{h})) = \sigma_{2}^{2} exp\left(-\frac{\|\mathbf{h}\|}{r_{2}}\right)$$

$$(4)$$

where r_1 and r_2 are scale parameters and σ_1^2 and σ_2^2 are stationary variances. The model also assumes the strong assumption $cov(\alpha_k(s), \alpha_l(s')) = 0$ for $k \neq l$.

R-squared and root mean squared error (RMSE) values were calculated to assess how well the data fit the AT-LST spatiotemporal model. A 10-fold cross-validation was performed to assess the accuracy of model predictions.

2.6. City-wide predictions

The fitted model is used to make predictions at unobserved locations. A space-time grid was defined using the centroid coordinates of the 120 m fishnet and the days when temperature data was collected. Using average LST for each of the fishnet cells and their locations as inputs, the model produced AT predictions and variances for all locations where LST was available across the city. Further, we compared the AT predictions to the remotely sensed LST by subtracting LST from the predicted AT. Final figures were produced in ArcGIS Pro. All collected AT and LST data as well as code for the spatiotemporal model are available on Mendeley Data (Scolio et al., 2023).

3. Results

3.1. ST and AT data collection

In total, there were 430 data points used to find cells with multiple measurements, and the cells contained anywhere from 2 to 5 data points. Altogether, 172 cells containing data points from at least two different days were used in this analysis (Fig. 2).

A univariate Moran's I test was used to assess spatial autocorrelation for both the AT and LST data used in the model (Table 1). All days show moderate to high Moran's I values except for August 29th. This day only contained 4 viable data points due to cloud cover interference which likely biased the results. These results suggest moderate to high levels of clustering in the data as expected and support the need to address spatial autocorrelation in the modeling approach. Overall, the AT data has a higher Moran's I value than LST. This could be because remotely sensed LST includes temperature measurements from a variety of different surfaces like green-spaces and pavement that have different thermodynamic qualities.

3.2. Model comparisons

The spatiotemporal model outperformed other models commonly used for temperature modeling. Table 2 compares the spatiotemporal model's performance to that of OLS, Spatial Lag, and Spatial Error models.

It should be noted that OLS does not account for spatial or temporal dependence in the data, making this approach inadequate.

Table 1
Moran's I test results for all days of data used in the AT-LST spatiotemporal model for both LST and AT. *August 29th, 2022 only contained 4 viable datapoints due to cloud cover interference, so these results may be biased by lack of data availability.

| | August 13 | August 29* | September 14 | April 2 | April 10 | June 5 |
|-----|-----------|------------|--------------|---------|----------|--------|
| LST | 0.259 | -0.205 | 0.639 | 0.398 | 0.464 | 0.326 |
| AT | 0.724 | 0.509 | 0.355 | 0.463 | 0.717 | 0.771 |

Table 2Model performance comparisons between spatiotemporal model and three other commonly used models. The spatiotemporal model outperformed all other models in terms of r-squared and RMSE. These values highlight the increased accuracy of predictions by the spatiotemporal model.

| Model | R-Squared | LST Coefficient | Standard Error | RMSE |
|----------------------|-----------|-----------------|----------------|----------|
| Spatiotemporal Model | 0.99 | -0.07 | 0.02 | 0.89 °C. |
| OLS | 0.80 | 0.85 | 0.02 | 3.54 °C |
| Spatial Lag | 0.81 | 0.85 | 0.02 | 3.82 °C |
| Spatial Error | 0.88 | 0.82 | 0.05 | 3.58 °C |

Spatial lag and spatial error models assume spatial dependence in the data but not temporal dependence also limiting their usefulness in modeling temperature.

Nevertheless, these three models all had relatively high r-squared values (r > 0.80) despite failing to account for autocorrelation in the data. The spatial error model outperformed the spatial lag model which was unexpected as spatial dependence for both LST and AT is directly affected by location. These results could suggest a prevalence of random effects that the spatial lag model fails to account for.

As shown in Table 2, the OLS, spatial lag, and spatial error models had a positive coefficient for the LST parameter, while the spatiotemporal model had a much smaller negative coefficient. These results indicate that, when spatial and temporal dependence and variability are accounted for, the direction of the LST effect on AT is changed and the magnitude is smaller. These results suggest that the relationship between LST and AT is highly influenced by spatial and temporal autocorrelation.

3.3. Model performance assessment

The spatiotemporal model resulted in an r-squared value of 0.99 and a RMSE of 0.89 °C. Fig. 3 depicts graphs for all viable data collection days comparing observed AT and predicted AT by the spatiotemporal model as well as 95% confidence intervals for the predicted AT given in °C. Notice that the scales of the charts vary to show the fit as weather conditions also varied across the data collections days. The model was able to accurately predict AT with 95% confidence for each day for the 120-m cells containing data from that day (Fig. 3).

This model was evaluated using a 10-fold cross-validation test. The cross-validation test yielded an r-squared value of 0.98 and a RMSE value of 0.98 and a RMSE value of 0.98 are cross-validated results produced 0.98 coverage of the 0.98 confidence interval meaning that 411 out of 430 predictions were withing the 0.98 CI. Comparisons between observed AT and the cross-validated predictions are shown in Fig. 4. The cross-validated comparisons show similar levels of variation between observed and predicted values when compared to the original spatiotemporal model using the full dataset. Further, these results do not flag any concerns for bias or overfitting of the model.

3.4. LST parameter performance

LST was the only spatiotemporal covariate used in the model in order to highlight the relationship between LST and AT. Using the spatiotemporal model, the parameter for LST gamma.st, given as β in the model specifications in eq. 3, was found to be a viable predictor for AT due to its significant t-statistic of -2.83. Typically, if a t statistic has an absolute value above or equal to 2, it is considered statistically significant. Therefore, LST is a significant predictor for AT in the model. The parameter estimations for the spatiotemporal model are presented in Table 3.

The gamma.st parameter is the only parameter that is non-latent and valuable for interpretation as it does not change with location or day. The gamma.st represents the underlying relationship between AT and ST, after accounting for all the temporal/spatial variations and correlations. The coefficient estimate for this parameter is -0.07 indicating a small negative relationship between LST and AT. While controlling other factors in the model, as LST increases, AT tends to decrease.

Fig. 5 provides a comparison of model parameter estimates from the original model using the full dataset with parameter estimates from the cross-validation. Overall, cross-validation parameter estimates were consistent with model parameter estimates showing reasonable agreement with regards to values and uncertainties. Importantly, the gamma.st parameter receives similar estimated values consistently across all groups indicating the validity of the observed relationship between LST and AT using the spatiotemporal model.

 Table 3

 Estimates and relevant statistics for model parameters.

| Parameter | Estimate | Standard error | t-Statistic |
|-------------------------------|----------|----------------|-------------|
| gamma.st | -0.07 | 0.02 | -2.83 |
| alpha.const.(Intercept) | 28.45 | 2.02 | 14.02 |
| alpha.V1.(Intercept) | 9.77 | 0.44 | 21.99 |
| log.range.const.exp | -2.14 | 0.92 | -2.31 |
| log. Sill.const.exp | 1.88 | 0.89 | 2.12 |
| log.range.V1.exp | -3.75 | 0.54 | -6.90 |
| log.sill.V1.exp | -0.18 | 0.46 | -0.40 |
| nu.log.nugget.(Intercept).iid | 0.02 | 0.08 | 0.23 |

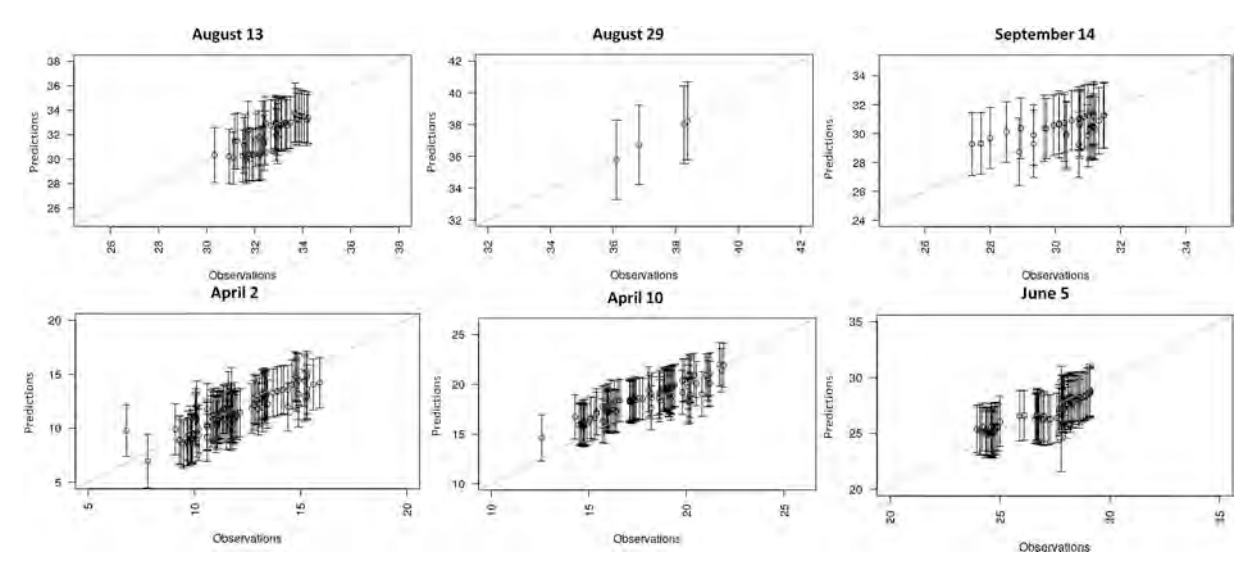


Fig. 3. Comparison of observed and predicted AT across the six data collection days in °C with 95% confidence intervals. A line with a slope of one and intercepts at (0,0) is used to demonstrate the strength of the relationship between observed and predicted values.

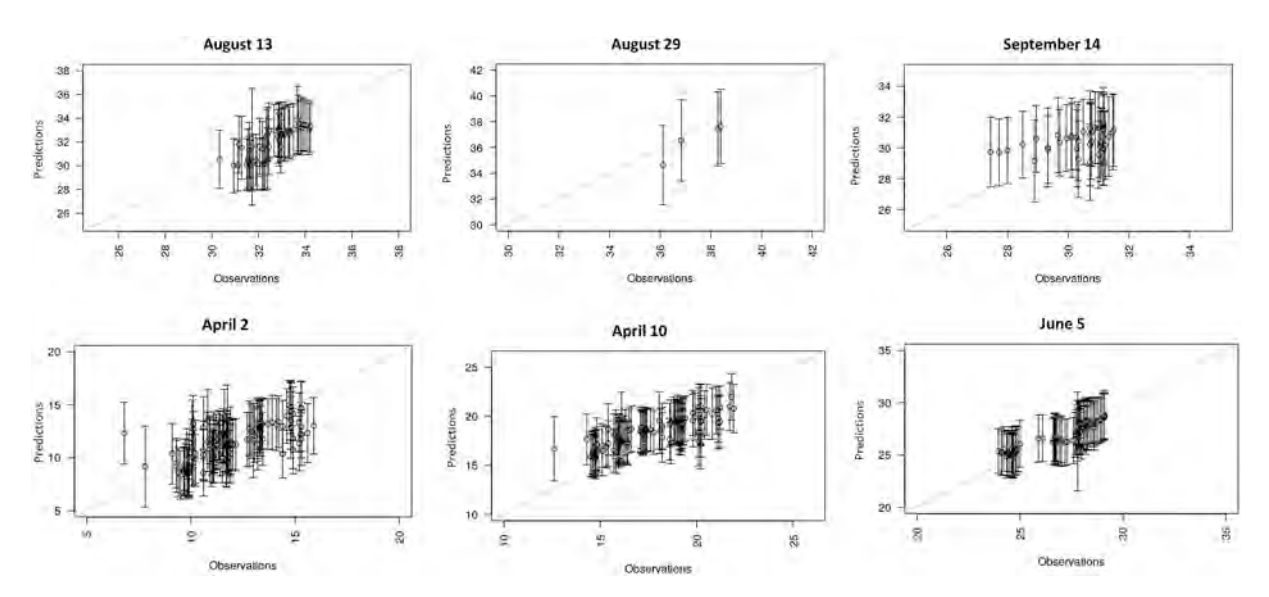


Fig. 4. Comparison of observed AT and predicted AT by the cross-validated model for the six data collection days in °C. 95% confidence intervals are shown. A line with a slope of one and intercepts at (0,0) is used to demonstrate the strength of the relationship between observed and predicted values

3.5. City-wide predictions

AT predictions were produced for all locations where LST was available for the days when temperature data was collected. Fig. 6 depicts the spatial distribution of AT predictions across Philadelphia. The model's predicted AT values highlight north and north-eastern Philadelphia as being consistently hotter than the rest of the city across all 6 days. Even on days where minimal AT observations were available (such as August 29th, 2022, where only 4 viable AT observations were used) the model was able to produce robust predictions across the city. The standard deviations of AT predictions at unobserved locations tend to become lower when those locations get closer to where the actual AT observations were collected. Overall, the standard deviations of AT predictions tend to be smaller at the days with more AT observations than days with fewer observations.

The spatial distribution of the difference between predicted AT and LST is also shown in Fig. 6. For 99.35% of predictions, AT was cooler than LST. The magnitude of the differences varies based on time and location. The largest differences were observed in more densely developed areas such as south and west Philadelphia. LST was shown to be cooler than AT along riverbanks and greener areas of the city such as the Wissahickon Valley Park. Although the spatial distribution of LST and predicted AT were similar, the range of

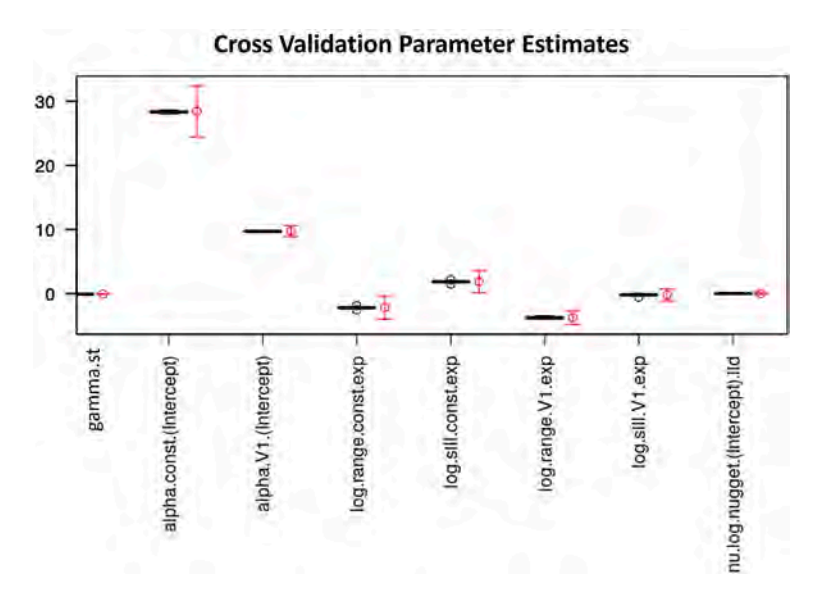


Fig. 5. Estimated parameters and approximate 95% confidence intervals (red) compared to parameter estimates from 10-fold cross-validation box plots (black). (For interpretation of the references to colour in this figure legend, the reader is referred to the web version of this article.)

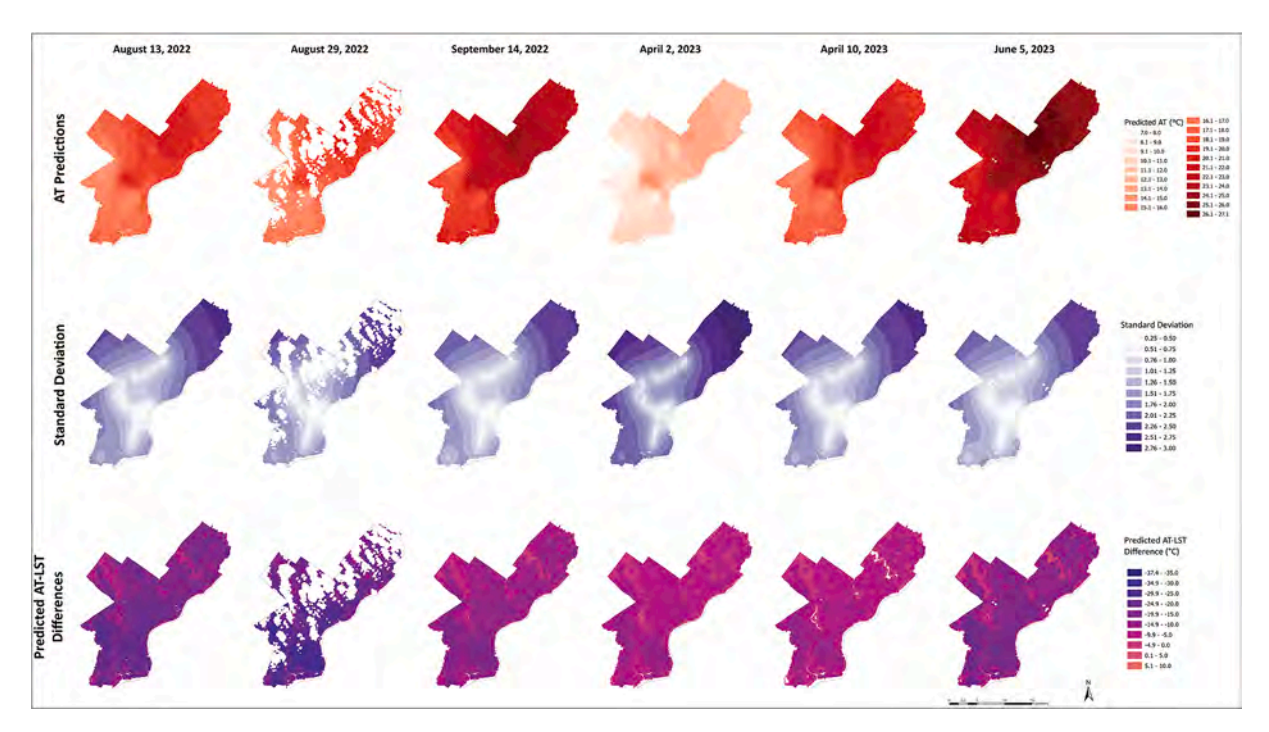


Fig. 6. City wide AT predictions and standard deviation for all data collection days as well as spatial representations of the difference between predicted AT and remotely sensed LST across the city.

Table 4 LST and Predicted AT ranges for each day in $^{\circ}$ C.

| Date | August 13, 2022 | August 29, 2022 | September 14, 2022 | April 2, 2023 | April 10, 2023 | June 5, 2023 |
|--------------|-----------------|-----------------|--------------------|---------------|----------------|--------------|
| LST | 20.69–50.34 | 27.58–54.61 | 18.28–48.16 | 2.62–29.06 | 11.66–41.50 | 23.24–52.72 |
| Predicted AT | 13.54–21.40 | 12.79–20.69 | 16.97–24.61 | 6.95–14.92 | 14.61–22.06 | 19.31–27.10 |

temperatures overall and across each day (Table 4) differed significantly. The model produced AT predictions ranging from $7.0\,^{\circ}$ C to $27.1\,^{\circ}$ C. However, the LST measurements used to create these predictions ranged from $2.62\,^{\circ}$ C to $54.61\,^{\circ}$ C further demonstrating that LST is not a reliable proxy for AT.

4. Discussion

In this paper, we study the nature of the relationship between LST and AT. We developed a model that can correct LST data to more closely reflect AT. To accomplish this, we pursue novel approaches to both air temperature data collection and LST-AT modeling. Previous papers have had inconsistent and contradictory findings on the nature of the relationship between LST and AT (Azevedo et al., 2016; Ho et al., 2016; Sheng et al., 2017; Yoo et al., 2018). Although, more recently, the body of literature supporting the presence of a relationship between LST and AT has grown significantly (Amani-Beni et al., 2022; do Nascimento, A. C. L., Galvani, E., Gobo, J. P. A., and Wollmann, C. A., 2022; Sfîcă, and Crețu, C.-Ștefănel, Ichim, P., Hriţac, R., and Breabăn, I.-G., 2023). Many papers look at this relationship in the context of the ability of LST to measure the urban heat island as compared to AT (Berg and Kucharik, 2022; Unger et al., 2010), but few are dedicated solely to investigating the nature of the AT-LST relationship.

This study produced empirical evidence of the relationship between remotely sensed LST and AT in urban areas by collecting AT data at the same time LST data is collected by satellite. Most often, previous studies have relied on spatially sporadic networks of stationary monitors to collect AT data during satellite pass over times (Berg and Kucharik, 2022; do Nascimento, A. C. L., Galvani, E., Gobo, J. P. A., and Wollmann, C. A., 2022; Flückiger et al., 2022; Liu et al., 2022; Sfică, and Creţu, C.-Ştefănel, Ichim, P., Hriţac, R., and Breabăn, I.-G., 2023; Wang et al., 2022). Because of the shortcomings of the most commonly used AT monitoring methods as discussed in the introduction, it has been hard to determine if the lack of consensus of understanding the AT- LST relationship is due to data limitations or the nature of the relationship.

We attempt to address the issue of spatial coverage using mobile monitoring methods which allows us to traverse a large portion of the city in the 4-h window around when the satellite passes overhead. We build off the work of other researchers who have utilized similar methods across varying scales. Unger et al. (2010) conducted car monitoring along a 12 km transect in Szeged, Hungary while LST was remotely sensed overhead using UAVs. Similar to the results presented here, this study found there to be a strong relationship between LST and AT (Unger et al., 2010). Amani-Beni et al. (2022) also found a significant correlation between LST and AT when using Landsat LST data and AT data that had been collected by bicycle at 6 different traverses in Beijing, China during a 6-h window around pass over times (Amani-Beni et al., 2022). The consistency of the results with this method and other similar methods suggests that the lack of consensus on the relationship between LST and AT could be due to the limited availability of high-quality AT data. Nevertheless, in cases where a high number and concentration of stationary monitors were used, such as in Switzerland (Flückiger et al., 2022), the Northeastern United States (Kloog et al., 2014), and Jingjinji area of China (C. Wang et al., 2022), strong LST and AT relationships have also been shown. Although it can be overcome through various data collection methods, these findings suggest that data quality and availability has been a significant limitation in understanding the LST-AT relationship.

Through the spatiotemporal model presented here, we have shown that LST can be used to model AT within 0.89 °C of accuracy. This model used LST as the only spatiotemporal covariate since remotely sensed LST is widely available for almost all locations around the world. While the study area of Philadelphia does have a fine scale land cover data set available, land cover was not included as a model covariate as the goal of the study was to explicitly investigate the AT-LST relationship as it is often presumed that remotely sensed LST is an adequate proxy for AT. An additional advantage to this approach is that this study can be easily replicated in other urban areas with varying geographic characteristics where fine scale land cover data is not available. Since our models performed very well as shown by their high r-squared values using only LST as a spatiotemporal covariate, adding in landcover was not warrented. Introducing additional model covariates creates greater potential for model overfitting, especially with the spatiotemporal model where r-squared equals 0.99, and would add undue complexity to the models, resulting in poor generalization of the models and increased computational costs. The spatiotemporal model differs from previous work in its use of temporal basis functions to account for spatial and temporal autocorrelation within the model itself. Addressing autocorrelation in the model framework instead of through sampling techniques means that the model can be compatible with datasets of different sizes. As established above, this flexibility is important due to the difficulties and limitations of AT data collection.

OLS, spatial lag, and spatial error models served as baselines for comparison for the spatiotemporal model. The presence of spatial and temporal dependence inherent to temperature data violates the foundational assumption of independence for OLS meaning that that model is not valid for use in this case. Spatial lag and spatial error models are commonly used models that account for spatial autocorrelation but do not address temporal autocorrelation. In terms of both standard and cross-validated r-squared as well as RMSE, the spatiotemporal model outperformed OLS, spatial lag, and spatial error models. These results demonstrate the impact of temporal dependence on the relationship between LST and AT as well as the importance of accounting for temporal dependence in modeling this relationship.

When compared to studies that use LST as the sole predictor for AT in either rural or urban environments (Bechtel et al., 2017; Goldblatt et al., 2021; Kloog et al., 2014; Parmentier et al., 2015; Rao et al., 2019; Zhu et al., 2013), R-squared and RMSE clearly demonstrate that our model is more accurate. For example, Rao et al.'s model predicts daily AT using LST across the entire Tibetan Plateau at a resolution of 0.05° x 0.05° with a maximum R-squared of 0.98 and RMSE of 1.87 °C (Rao et al., 2019). While our model outperforms most models that consider additional covariates to LST in AT predictions (Bechtel et al., 2017; dos Santos, 2020; Sandoval and Meza, 2014), improved RMSE have been produced by Alvi et al. (RMSE = 0.39–0.57 °C) who consider land cover and emissivity data in conjunction with LST as predictors in their model of 20 m² AT for Turku, Finland (Alvi et al., 2022). As previously stated, due to our models' high performance and our explicit aim of understanding the AT-LST relationship, investigating the impact of landcover

was beyond the scope of this paper. Including the work of Alvi et al., very few models that we are currently aware have been able to predict AT at as fine of a spatial scale as the one developed in this paper inhibiting their utility for urban temperature research and decision-making (Alvi et al., 2022; Bechtel et al., 2017; dos Santos, 2020).

The city-wide AT predictions highlight north and northeast Philadelphia as areas of the city that are consistently hotter than the rest of the city across all days that we produced predictions for regardless of weather conditions. Previous research using LST has identified north as well as south and west Philadelphia as areas that face higher temperatures in the city (Hammer et al., 2020; Hondula et al., 2012). We did not collect any AT measurements in west Philadelphia potentially biasing our ability to identify heat vulnerability in that neighborhood, but we did collect extensive AT measurements throughout south Philadelphia therefore giving more certainty to our map's results in that area. The largest differences between predicted AT and LST were identified in south and west Philadelphia which was not unexpected that these areas are highly urbanized and have limited greenspace and tree canopy coverage (Locke et al., 2023; Philly Tree Plan, 2023). This is in line with previous work that emphasizes how sensitive the LST-AT relationship is to physical context and shows that LST-AT differences are largest in densely developed areas with limited greenery (Berg and Kucharik, 2022; Gallo et al., 2011; Mutiibwa et al., 2015). The difference in temperature distribution between our predicted AT and previous LST based studies across Philadelphia illustrates how LST and AT tell different stories with regards to the near surface thermal environment.

LST has become dominant in the narrative that informs local governments, NGOs, and community organizations perceptions of urban heat distribution which in turn affects policymaking and implementation. For example, in Philadelphia, the city's comprehensive sustainability plan *Greenworks* uses LST data to highlight vulnerable neighborhoods to target with heat-related interventions (*Greenworks: A Vision for a Sustainable Philadelphia* | *Office of Sustainability*, 2016). Predictive models like the spatiotemporal model we employ have broad implications for research and policymaking by increasing access to high-quality data which better reflects the relationship between humans and the environment. A lack of appropriate environmental data can create a potential for environmental injustice wherein communities' lived experiences are contradicted by empirical data.

This study faced limitations with AT data collection, a prevalent issue with AT monitoring. We were only able to collect data on six different days, but increasing the number of observed days can help refine the estimation of temporal basis functions and improve the model's results. Since AT observations can only be measured at the exact location and time where the weather station is located, we collected data over a four-hour long period from 10:00 am to 2:00 pm EST. However, as the Landsat satellite pass-over time for Philadelphia occurs at 11:40 am EST, there is temperature variation throughout this period due to diurnal patterns of heating. The expanded time frame beyond the exact moment of the satellite pass is necessary to address the spatial distribution of heat within a heterogenous city and had been similarly pursued by others (Amani-Beni et al., 2022). Furthermore, our data collection days were limited to the beginning and end of summer and spring when weather is relatively temperate. However, previous research has shown that the relationship between AT and LST varies based on time of day (Cao et al., 2021; Cheval et al., 2022; Goldblatt et al., 2021; Shiflett et al., 2017), season (Cheval et al., 2022; Gallo et al., 2011; Zhang et al., 2014), location (Cao et al., 2021; Goldblatt et al., 2021; Mutiibwa et al., 2015; Unger et al., 2010) and scale (Cheval et al., 2022; Kloog et al., 2014; Sheng et al., 2017; Sohrabinia et al., 2015). Future research should test the spatiotemporal model and mobile monitoring methodologies under these conditions as well.

5. Conclusion

Due to being widely available, easily accessible, and having consistent spatial coverage, remotely sensed LST data is commonly used as a proxy for AT data. However, AT more accurately represents the ambient temperatures that humans actually experience meaning using uncorrected LST data in research and decision making has often been questioned (Berg and Kucharik, 2022; White, Newsome Jalonne L., Brines, S. J., Brown, D. G., Dvonch, J. T., Gronlund, C. J., Zhang, K., Oswald, E. M., and O, 'Neill Marie S., 2013). The goal of this research was to create a spatiotemporal model that uses LST data to predict AT that more accurately reflects the human experience of temperature. Our findings suggest that it is possible to use LST to predict AT within 0.89 °C of accuracy. Although previous research on this relationship varies, our results support the notion that there is a strong relationship between LST and AT and add empirical evidence to the growing body of literature addressing the LST-AT relationship in urban environments. In this study, we employ a novel data collection approach for AT data collection which allowed us to collect a large sample of AT data points using mobile monitoring. To overcome known limitations of non-linearity as well as spatial and temporal autocorrelation, a statistical model using temporal basis functions was employed allowing us to account for the spatial and temporal dependence that is intrinsic to temperature data from within the model's framework. This spatiotemporal model was used to create AT predictions across Philadelphia illustrating difference in range and spatial distributions of AT and LST across the city.

LST data is used to often guide policy and decision-making efforts in Philadelphia and elsewhere. City government, NGOs, and community organizations rely heavily on this imperfect data to inform their understanding of heat distribution across the city. AT data produced by the spatiotemporal model could have broad implications and utility for cities. Spatially explicit air temperature data is a critical component of the spatial support system that is necessary to promote holistic decision-making processes in the face of climate change. Ultimately, this model and the predictions produced can provide a better understanding of human-environment relations in an urban context by producing temperature data that more accurately represents the human experience.

Author contributions

Conceptualization: PK, YZ. Methodology MS, PK, YZ. Data Collection: MS, PK, KMS. Formal Data Analysis: MS, YZ, PK, KMS. Writing: MS, PK, YZ, KMS. Supervisions and Funding Acquisition: PK, YZ, MS.

CRediT authorship contribution statement

Madeline Scolio: Writing – review & editing, Writing – original draft, Validation, Project administration, Methodology, Investigation, Funding acquisition, Formal analysis. Peleg Kremer: Writing – review & editing, Writing – original draft, Supervision, Methodology, Investigation, Funding acquisition, Conceptualization. Yimin Zhang: Writing – review & editing, Validation, Methodology, Funding acquisition, Formal analysis, Conceptualization. Kabindra M. Shakya: Writing – review & editing, Methodology, Investigation, Formal analysis.

Declaration of competing interest

The authors declare the following financial interests/personal relationships which may be considered as potential competing interests:

Madeline Scolio reports financial support was provided by National Science Foundation. If there are other authors, they declare that they have no known competing financial interests or personal relationships that could have appeared to influence the work reported in this paper.

Data availability

Data will be made available on request.

Acknowledgements

This research was made possible by a supplemental grant from the National Science Foundation (Award Number 1832407).

References

- Alvi, U., Suomi, J., Käyhkö, J., 2022. A cost-effective method for producing spatially continuous high-resolution air temperature information in urban environments. Urban Clim. 42, 101123 https://doi.org/10.1016/j.uclim.2022.101123.
- Amani-Beni, M., Chen, Y., Vasileva, M., Zhang, B., Xie, G., 2022. Quantitative-spatial relationships between air and surface temperature, a proxy for microclimate studies in fine-scale intra-urban areas? Sustain. Cities Soc. 77, 103584 https://doi.org/10.1016/j.scs.2021.103584.
- Anselin, L., 1988. Spatial Econometrics: Methods and Models, vol. 4. Springer Science & Business Media.
- Azevedo, J.A., Chapman, L., Muller, C.L., 2016. Quantifying the daytime and night-time urban Heat Island in Birmingham, UK: A comparison of satellite derived land surface temperature and high resolution air temperature observations. Remote Sens. 8(2), Article 2 https://doi.org/10.3390/rs8020153.
- Bechtel, B., Zakšek, K., Oßenbrügge, J., Kaveckis, G., Böhner, J., 2017. Towards a satellite based monitoring of urban air temperatures. Sustain. Cities Soc. 34, 22–31. https://doi.org/10.1016/j.scs.2017.05.018.
- Berg, E., Kucharik, C., 2022. The dynamic relationship between air and land surface temperature within the Madison, Wisconsin urban Heat Island. Remote Sens. 14 (1) https://doi.org/10.3390/rs14010165. Article 1.
- Buyantuyev, A., Wu, J., 2010. Urban heat islands and landscape heterogeneity: linking spatiotemporal variations in surface temperatures to land-cover and socioeconomic patterns. Landsc. Ecol. 25 (1), 17–33. https://doi.org/10.1007/s10980-009-9402-4.
- Calvin, K., Dasgupta, D., Krinner, G., Mukherji, A., Thorne, P.W., Trisos, C., Romero, J., Aldunce, P., Barrett, K., Blanco, G., Cheung, W.W.L., Connors, S., Denton, F., Diongue-Niang, A., Dodman, D., Garschagen, M., Geden, O., Hayward, B., Jones, C., Péan, C., 2023. IPCC, 2023: Climate Change 2023: Synthesis Report. Contribution of Working Groups I, II and III to the Sixth Assessment Report of the Intergovernmental Panel on Climate Change [Core Writing Team, H. Lee and J. Romero (eds.)]. IPCC. Intergovernmental Panel on Climate Change (IPCC), Geneva, Switzerland. (First). https://doi.org/10.59327/IPCC/AR6-9789291691647.
- Cao, J., Zhou, W., Zheng, Z., Ren, T., Wang, W., 2021. Within-city spatial and temporal heterogeneity of air temperature and its relationship with land surface temperature. Landsc. Urban Plan. 206, 103979 https://doi.org/10.1016/j.landurbplan.2020.103979.
- Chakraborty, T., Venter, Z.S., Qian, Y., Lee, X., 2022. Lower urban humidity moderates outdoor heat stress. AGU Adv 3 (5). https://doi.org/10.1029/2022AV000729 e2022AV000729.
- Cheval, S., Dumitrescu, A., Iraşoc, A., Paraschiv, M.-G., Perry, M., Ghent, D., 2022. MODIS-based climatology of the surface urban Heat Island at country scale (Romania). Urban Clim. 41, 101056 https://doi.org/10.1016/j.uclim.2021.101056.
- Cliff, A.D., Ord, J.K., 1973. Spatial Autoregression. Economics 40 (2), 197-210.
- Di Cecco, G.J., Gouhier, T.C., 2018. Increased spatial and temporal autocorrelation of temperature under climate change. Sci. Rep. 8(1), Article 1 https://doi.org/10.1038/s41598-018-33217-0.
- do Nascimento, A. C. L., Galvani, E., Gobo, J. P. A., & Wollmann, C. A., 2022. Comparison between air temperature and land surface temperature for the City of São Paulo Brazil. Atmosphere 13 (3). https://doi.org/10.3390/atmos13030491. Article 3.
- dos Santos, R.S., 2020. Estimating spatio-temporal air temperature in London (UK) using machine learning and earth observation satellite data. Int. J. Appl. Earth Obs. Geoinf. 88, 102066 https://doi.org/10.1016/j.jag.2020.102066.
- Dwyer, J.L., Roy, D.P., Sauer, B., Jenkerson, C.B., Zhang, H.K., Lymburner, L., 2018. Analysis ready data: enabling analysis of the Landsat archive. Remote Sens. 10 (9), 1363. https://doi.org/10.3390/rs10091363.
- Emamifar, S., Rahimikhoob, A., Noroozi, A.A., 2013. Daily mean air temperature estimation from MODIS land surface temperature products based on M5 model tree. Int. J. Climatol. 33 (15), 3174–3181. https://doi.org/10.1002/joc.3655.
- Flückiger, B., Kloog, I., Ragettli, M.S., Eeftens, M., Röösli, M., de Hoogh, K., 2022. Modelling daily air temperature at a fine spatial resolution dealing with challenging meteorological phenomena and topography in Switzerland. Int. J. Climatol. 42 (12), 6413–6428. https://doi.org/10.1002/joc.7597.
- Fuentes, M., Guttorp, P., Sampson, P.D., 2006. Using transforms to analyze space-time processes. In: Statistical Methods for Spatio-Temporal Systems. CRC/Chapman and Hall, pp. 77–150.
- Gallo, K., Tarpley, D., Yu, Y., 2011. Evaluation of the relationship between air and land surface temperature under clear and cloudy-sky conditions. J. Appl. Meteorol. Climatol. 50 https://doi.org/10.1175/2010JAMC2460.1.
- Goldblatt, R., Addas, A., Crull, D., Maghrabi, A., Levin, G.G., Rubinyi, S., 2021. Remotely sensed derived land surface temperature (LST) as a proxy for air temperature and thermal comfort at a small geographical scale. Land 10 (4), Article 4. https://doi.org/10.3390/land10040410.
- Greene, S., Kalkstein, L.S., Mills, D.M., Samenow, J., 2011. An Examination of Climate Change on Extreme Heat Events and Climate–Mortality Relationships in Large U.S. Cities. Weather, Climate, and Society 3 (4), 281–292. https://doi.org/10.1175/WCAS-D-11-00055.1.

Greenworks: A Vision for a Sustainable Philadelphia | Office of Sustainability. (2016). City of Philadelphia. Retrieved November 19, 2022, from https://www.phila.gov/documents/greenworks-a-vision-for-a-sustainable-philadelphia/.

- Griffith, D.A., 2010. Modeling spatio-temporal relationships: retrospect and prospect. J. Geogr. Syst. 12 (2), 111–123. https://doi.org/10.1007/s10109-010-0120-x. Hammer, J., Ruggieri, D.G., Thomas, C., Caum, J., 2020. Local extreme heat planning: an interactive tool to examine a heat vulnerability index for Philadelphia, Pennsylvania. J. Urban Health 97 (4), 519–528. https://doi.org/10.1007/s11524-020-00443-9.
- Harlan, S.L., Ruddell, D.M., 2011. Climate change and health in cities: impacts of heat and air pollution and potential co-benefits from mitigation and adaptation. Curr. Opin. Environ. Sustain. 3 (3), 126–134. https://doi.org/10.1016/j.cosust.2011.01.001.
- Ho, H.C., Knudby, A., Xu, Y., Hodul, M., Aminipouri, M., 2016. A comparison of urban heat islands mapped using skin temperature, air temperature, and apparent temperature (Humidex), for the greater Vancouver area. Sci. Total Environ. 544, 929–938. https://doi.org/10.1016/j.scitotenv.2015.12.021.
- Hondula, D.M., Davis, R.E., 2014. The predictability of high-risk zones for heat-related mortality in seven US cities. Nat. Hazards 74 (2), 771–788. https://doi.org/10.1007/s11069-014-1213-5.
- Hondula, D.M., Davis, R.E., Leisten, M.J., Saha, M.V., Veazey, L.M., Wegner, C.R., 2012. Fine-scale spatial variability of heat-related mortality in Philadelphia County, USA, from 1983-2008: A case-series analysis. Environ. Health 11 (1), 16. https://doi.org/10.1186/1476-069X-11-16.
- Huang, K., Li, X., Liu, X., Seto, K.C., 2019. Projecting global urban land expansion and heat island intensification through 2050. Environ. Res. Lett. 14 (11), 114037 https://doi.org/10.1088/1748-9326/ab4b71.
- Julien, Y., Sobrino, J.A., Mattar, C., Ruescas, A.B., Jiménez-Muñoz, J.C., Sòria, G., Hidalgo, V., Atitar, M., Franch, B., Cuenca, J., 2011. Temporal analysis of normalized difference vegetation index (NDVI) and land surface temperature (LST) parameters to detect changes in the Iberian land cover between 1981 and 2001. Int. J. Remote Sens. 32 (7), 2057–2068. https://doi.org/10.1080/01431161003762363.
- Kloog, I., Nordio, F., Coull, B.A., Schwartz, J., 2014. Predicting spatiotemporal mean air temperature using MODIS satellite surface temperature measurements across the northeastern USA. Remote Sens. Environ. 150, 132–139. https://doi.org/10.1016/j.rse.2014.04.024.
- Landsat 9 Bands, 2021, November 30. NASA Landsat Science. https://landsat.gsfc.nasa.gov/satellites/landsat-9-instruments/landsat-9-spectral-specifications/.
- Landsat Science Products, 2023. USGS. https://www.usgs.gov/landsat-missions/landsat-science-products.
- Lemoine-Rodríguez, R., Inostroza, L., Zepp, H., 2022. Does urban climate follow urban form? Analysing intraurban LST trajectories versus urban form trends in 3 cities with different background climates. Sci. Total Environ. 830, 154570 https://doi.org/10.1016/j.scitotenv.2022.154570.
- Li, X., Li, W., Middel, A., Harlan, S.L., Brazel, A.J., Turner, B.L., 2016. Remote sensing of the surface urban heat island and land architecture in Phoenix, Arizona: combined effects of land composition and configuration and cadastral–demographic–economic factors. Remote Sens. Environ. 174, 233–243. https://doi.org/10.1016/j.rse.2015.12.022.
- Lindström, J., Szpiro, A., Sampson, P., Bergen, S., Sheppard, L., 2013. SpatioTemporal: An R Package for Spatio-Temporal Modelling of Air-Pollution. https://www.semanticscholar.org/paper/SpatioTemporal-%3A-An-R-Package-for-Spatio-Temporal-Lindstr%C3%B6m-Szpiro/d11cc8f4ff7507e0a3575b9ebdd6623ec3c06104.
- Liu, K., Su, H., Li, X., Wang, W., Yang, L., Liang, H., 2016. Quantifying Spatial—Temporal Pattern of Urban Heat Island in Beijing: An Improved Assessment Using Land Surface Temperature (LST) Time Series Observations From LANDSAT, MODIS, and Chinese New Satellite GaoFen-1. IEEE Journal of Selected Topics in Applied Earth Observations and Remote Sensing 9 (5), 2028–2042. https://doi.org/10.1109/JSTARS.2015.2513598.
- Liu, J., Hagan, D.F.T., Holmes, T.R., Liu, Y., 2022. An analysis of Spatio-temporal relationship between satellite-based land surface temperature and station-based near-surface air temperature over Brazil. Remote Sens. 14 (17) https://doi.org/10.3390/rs14174420. Article 17.
- Lloyd, C., 2021, November 30, Landsat 8 Bands, NASA Landsat Science, https://landsat.gsfc.nasa.gov/satellites/landsat-8-landsat-8-bands/.
- Locke, D.H., Roman, L.A., Henning, J.G., Healy, M., 2023. Four decades of urban land cover change in Philadelphia. Landsc. Urban Plan. 236, 104764 https://doi.org/10.1016/j.landurbplan.2023.104764.
- Meili, Naika & Manoli, Gabriele & Burlando, Paolo & Chow, Winston & Coutts, Andrew & Roth, Matthias & Velasco, Erik & Vivoni, Enrique & Fatichi, Simone. (2021). Tree effects on urban microclimate: Diurnal, seasonal, and climatic temperature differences explained by separating radiation, evapotranspiration, and roughness effects. Urban Forestry & Urban Greening. 58. 126970. https://doi.org/10.1016/j.ufug.2020.126970.
- Mitz, E., Kremer, P., Larondelle, N., Stewart, J.D., 2021. Structure of urban landscape and surface temperature: A case study in Philadelphia, PA. Front. Environ. Sci. 9 https://doi.org/10.3389/fenvs.2021.592716.
- Mumtaz, F., Tao, Y., de Leeuw, G., Zhao, L., Fan, C., Elnashar, A., Bashir, B., Wang, G., Li, L., Naeem, S., Arshad, A., Wang, D., 2020. Modeling Spatio-temporal land transformation and its associated impacts on land surface temperature (LST). Remote Sens. 12 (18) https://doi.org/10.3390/rs12182987. Article 18.
- Mutiibwa, D., Strachan, S., Albright, T., 2015. Land surface temperature and surface air temperature in complex terrain. IEEE J. Selected Top. Appl. Earth Observ. Remote Sens. 8 (10), 4762–4774. https://doi.org/10.1109/JSTARS.2015.2468594.
- Naserikia, M., Hart, M.A., Nazarian, N., Bechtel, B., Lipson, M., Nice, K.A., 2023. Land surface and air temperature dynamics: the role of urban form and seasonality. Sci. Total Environ. 905, 167306 https://doi.org/10.1016/j.scitotenv.2023.167306.
- Navarro-Estupiñan, J., Robles-Morua, A., Díaz-Caravantes, R., Vivoni, E.R., 2020. Heat risk mapping through spatial analysis of remotely-sensed data and socioeconomic vulnerability in Hermosillo, México. Urban Clim. 31, 100576 https://doi.org/10.1016/j.uclim.2019.100576.
- Nowak, D.J., Bodine, A.R., Hoehn, R., Ellis, A., Low, S.C., Roman, L.A., Henning, J.G., Stephan, E., Taggert, T., Endreny, T., 2016. The urban forests of Philadelphia. In: Resource Bulletin NRS-106. Newtown Square, PA: U.S. Department of Agriculture, Forest Service, Northern Research Station. 80 p, 106, pp. 1–80. https://doi.org/10.2737/NRS-RB-106.
- Parmentier, B., Mcgill, B., Wilson, A., Regetz, J., Jetz, W., Robert, G., Tuanmu, M.-N., Schildhauer, M., 2015. Using multi-timescale methods and satellite-derived land surface temperature for the interpolation of daily maximum air temperature in Oregon. Int. J. Climatol. 35 https://doi.org/10.1002/joc.4251.
- Pearsall, H., 2017. Staying cool in the compact city: vacant land and urban heating in Philadelphia, Pennsylvania. Appl. Geogr. 79, 84–92. https://doi.org/10.1016/j.apgeog.2016.12.010.
- Pepin, N., Deng, H., Zhang, F., Kang, S., Yao, T., 2019. An examination of temperature trends at high elevations across the Tibetan plateau: the use of MODIS LST to understand patterns of elevation-dependent warming. J. Geophys. Res. Atmos. 124 (11), 5738–5756. https://doi.org/10.1029/2018JD029798. Philly Tree Plan: Growing Our Urban Forest, 2023. https://www.phila.gov/media/20230223005617/Philly-Tree-Plan.pdf.
- 2019 Modeled Landscape Change: Philadelphia 1900-2100. USGS, 2019. https://www.usgs.gov/media/images/philadelphia-1900-2100.
- QuickFacts: Philadelphia City, Pennsylvania, 2022. U.S. Census Bureau. https://www.census.gov/quickfacts/philadelphiacitypennsylvania.
- Rao, Y., Liang, S., Wang, D., Yu, Y., Song, Z., Zhou, Y., Shen, M., Xu, B., 2019. Estimating daily average surface air temperature using satellite land surface temperature and top-of-atmosphere radiation products over the Tibetan Plateau. Remote Sens. Environ. 234, 111462 https://doi.org/10.1016/j.rse.2019.111462.
- Sandoval, Eduardo Bustos, Meza, Francisco J., 2014. A method to estimate maximum and minimum air temperature using MODIS surface temperature and vegetation data: application to the Maipo Basin, Chile. Theor. Appl. Climatol. 120 (1–2), 211–226. https://doi.org/10.1007/s00704-014-1167-2.
- Savić, S., Šećerov, I., Lalić, B., Nie, D., Roantree, M., 2023. Air temperature and relative humidity datasets from an urban meteorological network in the City area of Novi Sad (Serbia). Data Brief 49. https://doi.org/10.1016/j.dib.2023.109425.
- Schinasi, L.H., Kanungo, C., Christman, Z., Barber, S., Tabb, L., Headen, I., 2022. Associations between historical redlining and present-day heat vulnerability housing and land cover characteristics in Philadelphia, PA. J. Urban Health 99 (1), 134–145. https://doi.org/10.1007/s11524-021-00602-6.
- Schwarz, K, Fragkias, M, Boone, CG, Zhou, W, McHale, M, Grove, JM, et al., 2015. Trees Grow on Money: Urban Tree Canopy Cover and Environmental Justice. PLoS ONE 10 (4), e0122051. https://doi.org/10.1371/journal.pone.0122051.
- Schwarz, N., Schlink, U., Franck, U., Großmann, K., 2012. Relationship of land surface and air temperatures and its implications for quantifying urban heat island indicators—an application for the city of Leipzig (Germany). Ecol. Indic. 18, 693–704. https://doi.org/10.1016/j.ecolind.2012.01.001.
- Scolio, M., Kremer, P., Zhang, Y., Shakya, K., 2023. Spatial-temporal modeling of the relationship between surface temperature and air temperature in metropolitan Urban Systems (version V1) [dataset]. Mendeley Data. https://doi.org/10.17632/yk9g44bdnd.1.
- Sfīcă, L., Creţu, C.-Ştefănel, Ichim, P., Hriţac, R., & Breabăn, I.-G., 2023. Surface urban heat island of Iași city (Romania) and its differences from in situ screen-level air temperature measurements. Sustain. Cities Soc. 94, 104568 https://doi.org/10.1016/j.scs.2023.104568.

Shade, C., Kremer, P., 2019. Predicting land use changes in Philadelphia following green infrastructure policies. Land 8(2), Article 2. https://doi.org/10.3390/

- Sheng, L., Tang, X., You, H., Gu, Q., Hu, H., 2017. Comparison of the urban heat island intensity quantified by using air temperature and Landsat land surface temperature in Hangzhou, China. Ecol. Indic. 72, 738–746. https://doi.org/10.1016/j.ecolind.2016.09.009.
- Shiflett, S.A., Liang, L.L., Crum, S.M., Feyisa, G.L., Wang, J., Jenerette, G.D., 2017. Variation in the urban vegetation, surface temperature, air temperature nexus. Sci. Total Environ. 579, 495–505. https://doi.org/10.1016/j.scitotenv.2016.11.069.
- Sohrabinia, M., Zawar-Reza, P., Rack, W., 2015. Spatio-temporal analysis of the relationship between LST from MODIS and air temperature in New Zealand. Theor. Appl. Climatol. 119, 567–583. https://doi.org/10.1007/s00704-014-1106-2.
- Stewart, J.D., Kremer, P., 2022. Temporal change in relationships between urban structure and surface temperature. Environ. Plann. B: Urban Anal. City Sci. 49 (9), 2297–2311. https://doi.org/10.1177/23998083221083677.
- Stewart, I.D., Krayenhoff, E.S., Voogt, J.A., Lachapelle, J.A., Allen, M.A., Broadbent, A.M., 2021. Time evolution of the surface urban Heat Island. Earth's Future 9 (10). https://doi.org/10.1029/2021EF002178 e2021EF002178.
- Tobler, W.R., 1970. A computer movie simulating urban growth in the Detroit region. Econ. Geogr. 46, 234-240. https://doi.org/10.2307/143141.
- Unger, J., Gál, T., Rakonczai, J., Mucsi, L., Szatmari, J., Tobak, Z., Van Leeuwen, B., Fiala, K., 2010. Modeling of the urban heat island pattern based on the relationship between surface and air temperatures. Idojaras 114, 287–302.
- Ward, Michael & Gleditsch, Kristian. (2019). Spatial Regression Models. https://doi.org/10.4135/9781071802588.
- Wang, T., Shi, J., Ma, Y., Husi, L., Comyn-Platt, E., Ji, D., Zhao, T., Xiong, C., 2019. Recovering land surface temperature under cloudy skies considering the solar-cloud-satellite geometry: application to MODIS and Landsat-8 data. J. Geophys. Res. Atmos. 124 (6), 3401–3416. https://doi.org/10.1029/2018JD028976.
- Wang, C., Bi, X., Luan, Q., Li, Z., 2022. Estimation of daily and instantaneous near-surface air temperature from MODIS data using machine learning methods in the Jingjinji area of China. Remote Sens. 14(8), Article 8 https://doi.org/10.3390/rs14081916.
- Warren, E.L., Young, D.T., Chapman, L., Muller, C., Grimmond, C.S.B., Čai, X.-M., 2016. The Birmingham urban climate laboratory—A high density, urban meteorological dataset, from 2012–2014. Sci. Data 3 (1), 160038. https://doi.org/10.1038/sdata.2016.38.
- White, -Newsome Jalonne L., Brines, S. J., Brown, D. G., Dvonch, J. T., Gronlund, C. J., Zhang, K., Oswald, E. M., & O, 'Neill Marie S., 2013. Validating satellite-derived land surface temperature with in situ measurements: A public health perspective. Environ. Health Perspect. 121 (8), 925–931. https://doi.org/10.1289/ehp.1206176.
- White-Newsome, J., McCormick, S., Sampson, N., Buxton, M., O'Neill, M., Gronlund, C., Catalano, L., Conlon, K., Parker, E., 2014. Strategies to reduce the harmful effects of extreme heat events: A Four-City study. Int. J. Environ. Res. Public Health 11 (2), 1960–1988. https://doi.org/10.3390/ijerph110201960.
- Wikle, C.K., Zammit-Mangion, A., Cressie, N., 2019. Spatio-Temporal Statistics with. Chapman & Hall/CRC, Boca Raton, FL.
- Yoo, C., Im, J., Park, S., Quackenbush, L.J., 2018. Estimation of daily maximum and minimum air temperatures in urban landscapes using MODIS time series satellite data. ISPRS J. Photogramm. Remote Sens. 137, 149–162. https://doi.org/10.1016/j.isprsjprs.2018.01.018.
- Zhang, P., Bounoua, L., Imhoff, M., Wolfe, R., Thome, K., 2014. Comparison of MODIS land surface temperature and air temperature over the continental USA meteorological stations. Can. J. Remote. Sens. 40, 110–122. https://doi.org/10.1080/07038992.2014.935934.
- Zhu, W., Lű, A., Jia, S., 2013. Estimation of daily maximum and minimum air temperature using MODIS land surface temperature products. Remote Sens. Environ. 130, 62–73. https://doi.org/10.1016/j.rse.2012.10.034.
- Zhu, X., Duan, S.-B., Li, Z.-L., Wu, P., Wu, H., Zhao, W., Qian, Y., 2022. Reconstruction of land surface temperature under cloudy conditions from Landsat 8 data using annual temperature cycle model. Remote Sens. Environ. 281, 113261 https://doi.org/10.1016/j.rse.2022.113261.
- Ziter, C.D., Pedersen, E.J., Kucharik, C.J., Turner, M.G., 2019. Scale-dependent interactions between tree canopy cover and impervious surfaces reduce daytime urban heat during summer. Proc. Natl. Acad. Sci. 116 (15), 7575–7580. https://doi.org/10.1073/pnas.1817561116.